

CARABINER TESTING

Final Report

16.621

Spring 2001

Author: Marianne Okal

Advisors: Kim Blair and Dave Custer

Partner: Jonathan Graham

December 11, 2001

Contents

Abstract	3
1 Introduction	4
1.1 Motivation.....	5
2 Objective	5
3 Previous Work	5
4 In-Field Conditions and Loading Model	6
5 Technical Approach	8
5.1 Test Design & Overview.....	8
5.2 Test Apparatus.....	9
5.3 Experimental Approach.....	10
6 Results	12
6.1 Overview.....	12
6.2 Cyclic Failure.....	12
6.3 Deformation.....	14
6.4 Fracture Surface Analysis.....	19
7 Discussion	21
7.1 Cyclic Failure.....	21
7.2 Deformation.....	22
7.3 Fracture Surface Analysis.....	22
7.4 Proposed Fatigue Testing Standard.....	25
8 Conclusion	26
8.1 Future Work.....	27
Appendix A	30
Appendix B	32
Appendix C	34
Appendix D	36

List of Figures

1	D-shaped carabiner.....	4
2	Falling Climber.....	7
3	ASTM standard test apparatus in TELAC.....	10
4	Load vs. Cycles to Failure results.....	13
5	Load vs. Stroke for first and 200 th cycle of 0.5 - 20kN test	16
6	Load vs. Stroke for 233 rd and 9291 st cycles of a 0.5-8kN cyclic test	17
7	Load vs. strain for cycle 27 of a 20kN cyclic test.....	18
8	Load vs. strain for cycles 233 and 9291 of an 8kN cyclic test.....	18
9	Carabiner fracture surfaces for 12kN (a) and 8kN (b) load cycles	20
10	Stress vs. Crack Length for both open and closed gate testing	21
11	Kc vs. Stress values for both open and closed gate conditions	24
12	Proposed safety margin line for closed gate testing for Black Diamond Light D carabiners.....	26
A-1	Three-view of the main ASTM grips.....	30
A-2	Three-view of the connectors.....	31
B-1	Pin/carabiner free body diagram.....	32
C-1	Finite element analysis of a D-shaped carabiner.....	34

List of Tables

1	Test matrix for carabiner testing.....	11
2	Cyclic Failure results	14
3	Gate gap measurement values.....	15
4	Stress/crack size relationships for open and closed gate conditions.....	23
D-1	Raw Data Collected on Carabiners.....	36

Abstract

Carabiners are metal links that mountain climbers use to protect themselves from injury or death in the event of a fall. The American Society of Testing and Materials testing standard for carabiners is a single pull to failure. Because carabiners experience cyclic, dynamic loads in the field, the purpose of this study was to enhance the testing standards by determining their failure characteristics under these in-field condition loads. Three major tests were carried out. First, cyclic testing determined the lifetime of carabiners under different loads. The deformation characteristics were observed by taking measurements and X-ray photographs, and by placing strain gauges on the carabiners. Third, crack formation was monitored by taking a second type of X-ray photography and observing the fracture surface. The results of this study concluded that carabiners have a long lifetime, that most of their deformation occurs within the first few cycles of loading, and that significant cracks occur during loading. The results of this study also propose a new testing standard for carabiners that is representative of their in-field use.

1 Introduction

Carabiners (Figure 1) are metal links that mountain climbers use to protect themselves from injury or death in the event of a fall¹. One end of the carabiner is clipped around a piece of webbing that is attached to the mountainside, and the other end of the carabiner is clipped around a rope that is attached to the climber. It is important for climbers to know when a carabiner should be retired in order to avoid failure, which can lead to serious injury, or, in some cases, death.

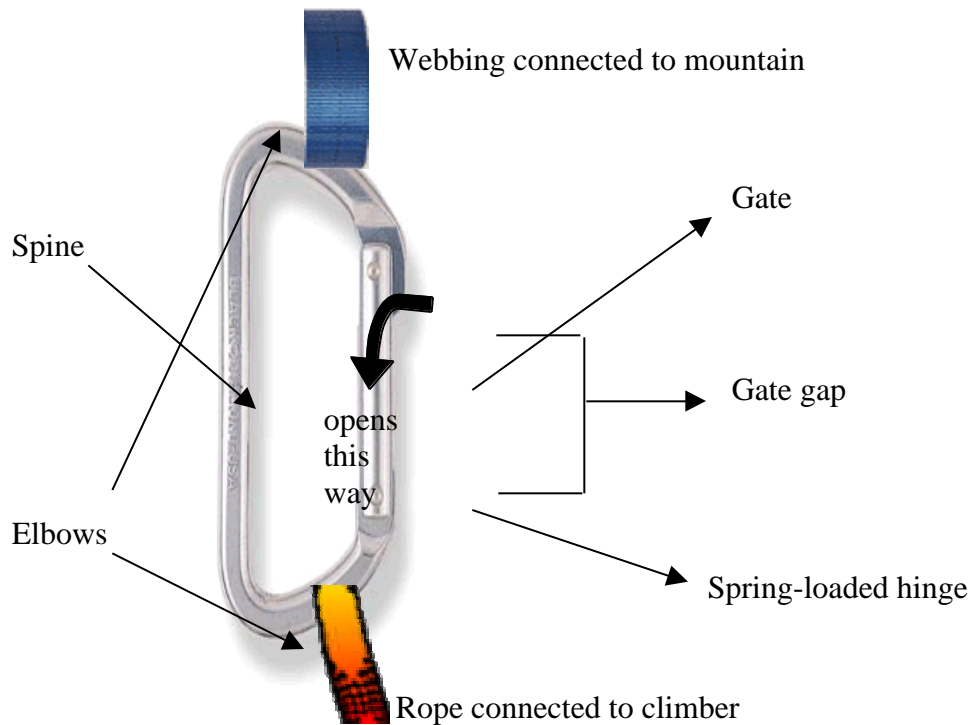


Figure 1. D-shaped carabiner (As found on Black Diamond Equipment website at http://www.blackdianondequipment.com/rockclimbing/biners_light_d.html)

Each carabiner is equipped with a spring-loaded gate that the climber opens to insert the rope or webbing. The most common type of carabiner is D-shaped, forged of

7075 aluminum alloy, and rated at a maximum tensile loading of 24kN.² Carabiners are designed to repeatedly withstand the loads of climbing falls, which are typically between 2 and 20kN, but in extreme cases can be as high as 20kN.

1.1 Motivation

The current testing and rating standard for carabiners, which was developed by the American Society of Testing and Materials (ASTM), does not test or rate carabiners for loads they experience in the field³. The current standard calls for carabiners to undergo a single pull to failure and rates them at the load at which they fail, usually around 24kN for closed gate testing and 7kN for open gate testing. Climbing falls typically load carabiners dynamically, as the stretching rope acts as a spring. Repeated falls result in cyclic loading. Additionally, the forces experienced in the field are between 2 and 20kN.⁴ The current testing and rating standard does not represent these conditions. The results may also serve to optimize future carabiner design.

2 Objective

The purpose of this study is to enhance the testing and rating standards of carabiners by determining their failure and deformation characteristics under loads reflecting their in-field use.

3 Previous Work

The previous work in this field is extremely limited, as little research has been conducted on carabiners. The most notable experiment loaded carabiners at a cyclic

loading of maximum amplitude 2kN, the lower end of the loading range⁵. The results of this test concluded that after more than 500,000 cycles on the carabiner, the gate gap was displaced by 1 μm . This data was valuable in providing a conservative approximation to the number of cycles to failure for carabiners at higher loads.

4 In-Field Conditions and Loading Model

The loading conditions carabiners experience in the field are described in this section and were used to determine the testing parameters. Climbers typically take numerous falls on carabiners, therefore repeatedly, or cyclically, loading them. Also, a variable that is not reflected in the current standard is the effect of the rope on carabiner loading. The rope that passes through a carabiner is designed to stretch when loaded in order to absorb the shock of the fall and reduce shock to the human body⁴. Hence, the rope can be modeled as a spring, implying a dynamic, sinusoidal loading.

On average, climbers load a rope 0.5 seconds during a fall. Hence, the period of this sinusoidal force is assumed to be 0.5 seconds⁴.

In the field, carabiners are also loaded in both open and closed gate configurations because the gate may accidentally open during a person's fall.

Finally, climber falls result in loads up to 12kN on the rope, which translates to a maximum force of 20kN on the carabiner⁴. This value is calculated in the following manner. The force exerted on a climber's body during his or her fall is related to the fall factor, F , of the fall. This value is defined as the ratio between the distance the climber falls to the length of the rope L . If the climber has placed his or her last carabiner d

meters below, then he or she will fall $2d$. Hence, $F = \frac{2d}{L}$. The worst-case scenario is a fall factor of 2, or when $d = L$.

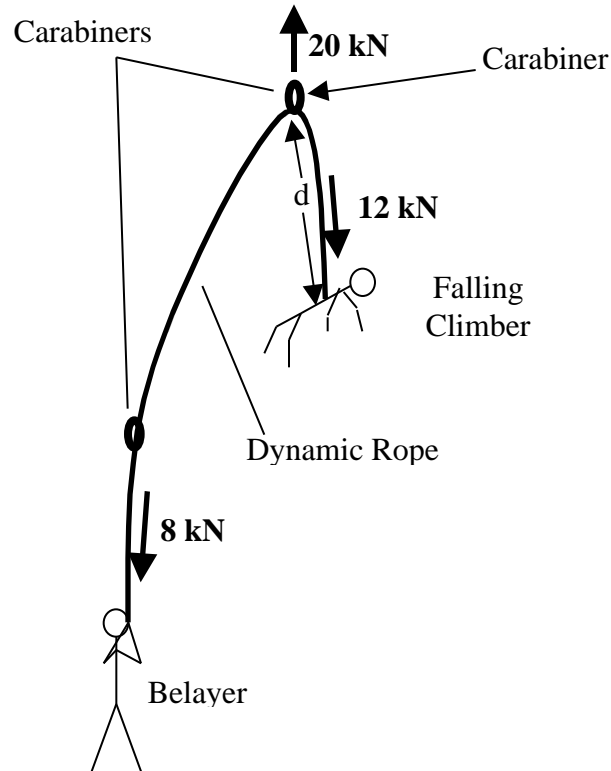


Figure 2. Falling climber. L is the length of the rope from the belayer to the falling climber.

Using energy methods, it is found that the force exerted on the climber's body is

$$T = Mg \left(1 + \sqrt{1 + \frac{2kF}{Mg}} \right)$$

where M is the mass of the climber, k is the modulus of the rope, and g is the acceleration due to gravity. For a 90kg (200 lb) climber enduring a factor 2 fall, and

using a standard rope with modulus $k = 30.0$ kN, $T = 12.71$ kN. About $1/3$ of this force is lost to friction between the rope and the carabiner and the stretch of the rope as it is loaded, and so the belayer, or the person on the ground holding the other end of the rope, only experiences $2/3$ of this force. Hence, using equilibrium, the carabiner experiences 1 and $2/3$ of the force exerted on the climber. For the worst-case scenario, the carabiner is loaded to approximately

$$12.7 \left(1\frac{2}{3}\right) = 21.1 \text{ kN}$$

In summary, the loads experienced by carabiners in the field are cyclic, dynamic, range up to 20kN in magnitude, and are experienced in both open and closed gate conditions.

5 Technical Approach

5.1 Test Design & Overview

Using the parameters described above, carabiners were tested to failure under cyclic, dynamic loads with a period of 0.5 seconds under both open and closed gate scenarios. Three major types of tests were conducted to characterize carabiner failure. In the first test, thirty-five carabiners were cycled to failure under dynamic loads. Approximately 75% of carabiners were loaded in closed gate conditions and the remainder were loaded in open gate conditions.

The second test tracked the carabiner deformation by taking X-ray pictures, placing strain gauges on carabiner spines, recording displacement data collected directly from the MTS machine clamps, and taking measurements of the gate gap displacement.

Finally, carabiners were tested both prior to and after failure for crack growth by taking X-ray pictures and measurements of the failure surface.

Black Diamond Light D carabiners were used for all tests as these carabiners are commonly used in the field. These carabiners are D-shaped, made of 7075 aluminum, and have single pull ratings of 24kN and 7kN under closed and open gate conditions, respectively⁶.

5.2 Test Apparatus

Figure 3 depicts the MTS tensile loading machine that was used to load the carabiners. The standard ASTM test apparatus was used in order to produce results compatible with current testing and rating methods. The test apparatus, shown in the blow-up of Figure 3, calls for each end of the carabiner to be clipped around a steel dowel with a 5 ± 0.05 mm radius³. Each pin is attached to a steel grip, which is in turn inserted into an MTS machine clamp. However, the MTS machine clamps available in the MIT Technology Laboratory for Advanced Composites (TELAC) are not compatible with the ASTM grip design. Hence, a connector piece was designed and machined to make the interface between the grips and the clamps. The pins, grips, and connectors are shown in Figure 3, and the engineering drawings for these parts are located in Appendix A.

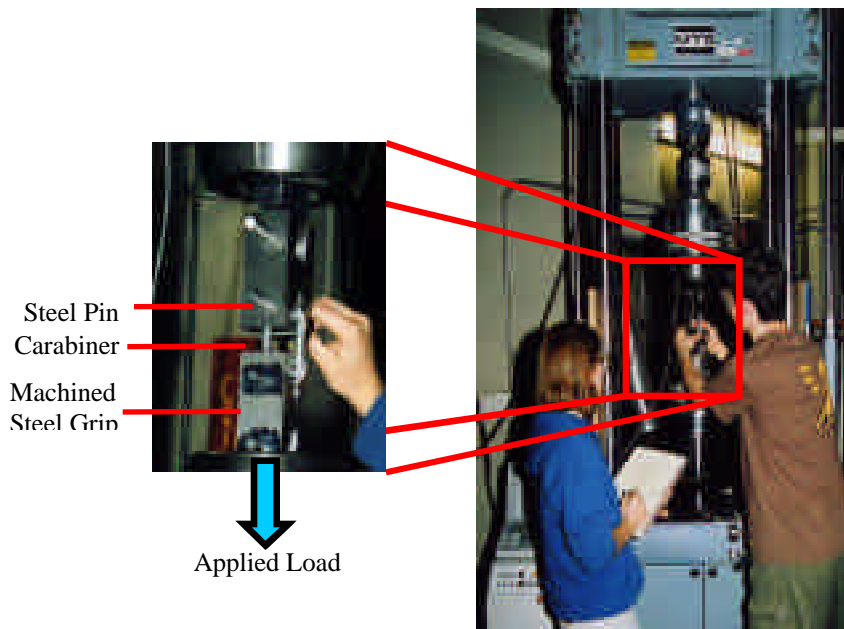


Figure 3. ASTM standard test apparatus in TELAC.

The MTS machine applies the cyclic, dynamic loading to the carabiners. A computer records the displacement, load, and time data. Appendix B describes errors associated with the MTS machine.

The X-ray pictures were taken on a Torrex 150D X-ray machine and the microscopic pictures of the carabiner fracture surface were taken on a Zeiss Stemi 2000-C microscope.

5.3 Experimental Approach

Carabiners were cycled to failure under both open and closed gate conditions and at the upper end of their load range, specifically from 8 to 20kN for closed gate and from 4 to 6 kN for open gate. Originally, 3 tests were planned for each configuration, but four

tests were conducted for most of the closed gate testing. The final test is matrix shown below, in Table 1. For each case, the cycles to failure was recorded.

Table 1. Test matrix for carabiner testing.

Cyclic Load Range [kN]	Closed Gate Testing	Open Gate Testing
0.5-4	-	3
0.5-5	-	3
0.5-6	-	3
0.5-8	3* [^]	-
0.5-10	3*	-
0.5-12	4*	-
0.5-14	4	-
0.5-16	4	-
0.5-18	4	-
0.5-20	4 [^]	-

* denotes at least one carabiner underwent X-ray photography

[^] denotes at least one carabiner equipped with a strain gauge on spine

The deformation of the carabiner was measured in four ways. For the 8kN and 20kN load cases, a strain gauge was placed on the carabiner’s spine. Displacement data was continuously fed to a computer. This same computer was also connected to the MTS machine and recorded the stroke, or displacement of the bottom MTS clamp. Since the top clamp remained fixed for all tests, this displacement was concluded to represent the carabiner’s deformation. Additionally, the length of the gate gap was periodically measured with a micrometer to determine if the carabiner deformation could be observed by a change in the gate gap size throughout the loading. Finally, short-exposure X-ray pictures were taken, at 8, 10, and 12kN tests, copied onto transparencies, and placed on top of each other to determine whether any significant deformation had occurred at various periods in the cycling.

Internal crack growth was monitored by taking long-exposure X-ray photography of the carabiners at the end of their lifetime, when it was suspected the cracks would begin to form. On average, the carabiners were X-rayed every 500 cycles. They were first soaked in iodine penetrant, a solution that seeps into cracks and therefore allows them to show up on X-ray photography⁷. These X-ray tests were only performed at 8 kN, as it was suspected previously that the crack propagation at higher loads would occur too quickly.

6 Results

6.1 Overview

The data collected led to a number of results regarding the failure characteristics of carabiners under in-field condition loads. One of the most significant results was the determination of an load vs. number of cycles to failure, or L-N, curve, which had yet to be found for carabiners. Other results were that most of carabiner deformation occurs within the first few cycles of loading and that even these deformations are so small that they are hardly, if at all, visible to the naked human eye or through X-ray photography. In addition, no cracks were observed by X-ray photography during cycling, but post-failure analysis of the fracture surface yielded results concerning the critical crack size of the carabiners. Appendix D lists all raw data.

6.2 Cyclic Failure

Data was collected on the number of cycles to failure, N_i , for each load condition and a general stress vs. N (L-N) curve was found. A total of 35 carabiners were tested

cyclically: 26 in closed-gate configurations, and 9 in open-gate situations. The results for the maximum load vs. cycles to failure are shown in the graph in Figure 4.

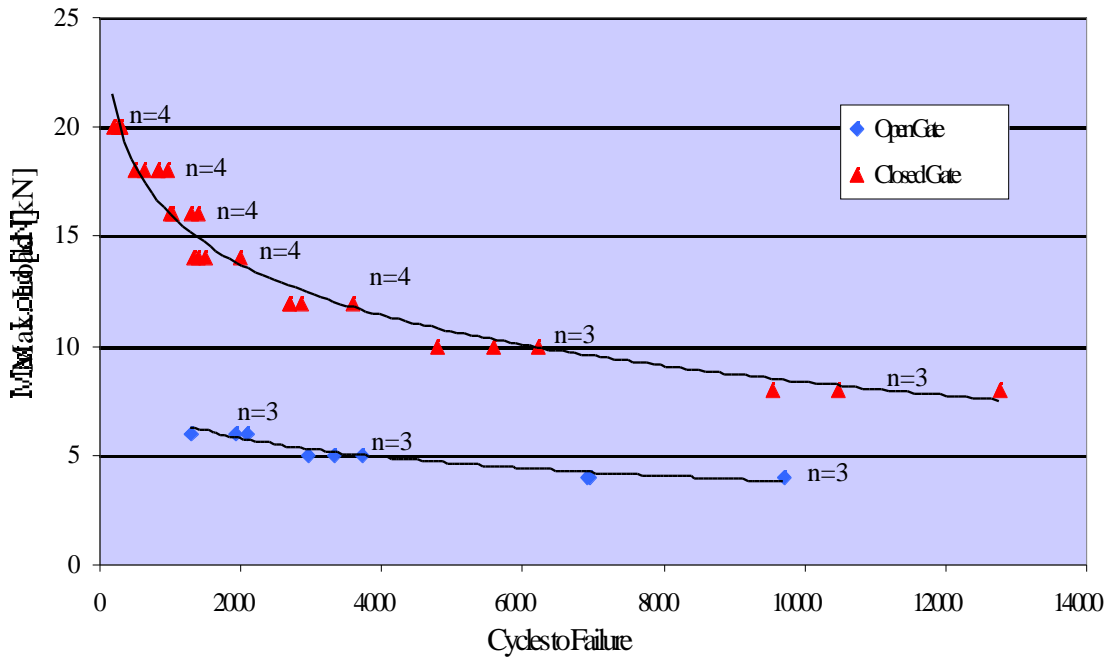


Figure 4. Load vs. Cycles to Failure results. n = number of carabiners tested for each condition.

The average number of cycles, range, and percent variation for each condition are shown in Table 2. The percent variation is defined as the ratio between the standard deviation and the average of a sample space. The standard deviation, SD, is equal to⁸

$$SD = \sqrt{\frac{(y_i - y_{mean})^2}{N - 1}}$$

where y_i is the cycles to failure, y_{mean} is the average cycles to failure, and N is the number of data points in the data set. The percent variation is therefore given by

$$\text{percent variation} = 100 \frac{SD}{y_{mean}}$$

Table 2: Cyclic Failure results

Cyclic Load Range [kM]	Average Cycles to Failure	Range of Cycles	Percent Variation [%]
0.5 – 4	7849	6901 - 9694	20.36
0.5 – 5	3351	2974 - 3740	11.46
0.5 – 6	1775	1309 - 2098	23.28
0.5 – 8	10939	9554 - 12775	15.15
0.5 – 10	5533	4785 - 6226	13.05
0.5 – 12	2959	2693 - 3608	20.07
0.5 – 14	1556	1340 - 1988	19.08
0.5 – 16	1182	989 – 1408	17.68
0.5 – 18	751	489 – 950	24.42
0.5 – 20	263	194 – 312	19.45

This table shows that the variation in the data is not dependent on the load at which the carabiners are cycled.

6.3 Deformation

Measurements taken early during the testing phase showed no significant change in the gate gap through the duration of the tests. The average displacement percentage is defined as one hundred times the ratio of the change in the gate gap size to the initial gate gap size, or

$$100 \frac{G_f - G_i}{G_i}$$

where G_f is the final gate gap and G_i is the initial gate gap. The value of the percentage for each load is shown in the table below.

Table 3: Gate gap measurement values.

Cyclic Load Range [kN]	Average Initial Gate Gap Measurement [mm]	Average Final Gate Gap Measurement [mm]	Gate Gap Displacement percentage [%]
0.5 – 8	28.10	28.15	0.00
0.5 – 10	28.00	28.13	0.54
0.5 – 12	28.10	28.14	0.14
0.5 – 14	28.00	28.30	1.07
0.5 – 16	28.00	28.30	1.07
0.5 – 18	28.10	28.27	0.60
0.5 – 20	28.16	30.75	3.47

The short-exposure X-ray pictures taken as the carabiners were cycled were transferred to transparencies, and these transparencies were laid on top of each other to look for any shape mismatches. It was found that there were no significant results or deformations.

The deformation data collected from the MTS machine, or stroke data (see Section 5.3), showed that most of a carabiner's deformation at higher loads occurs within the first few cycles of loading. Figure 5 shows this behavior for a cyclic test at 20kN. The 1st and 200th cycles are shown for comparison.

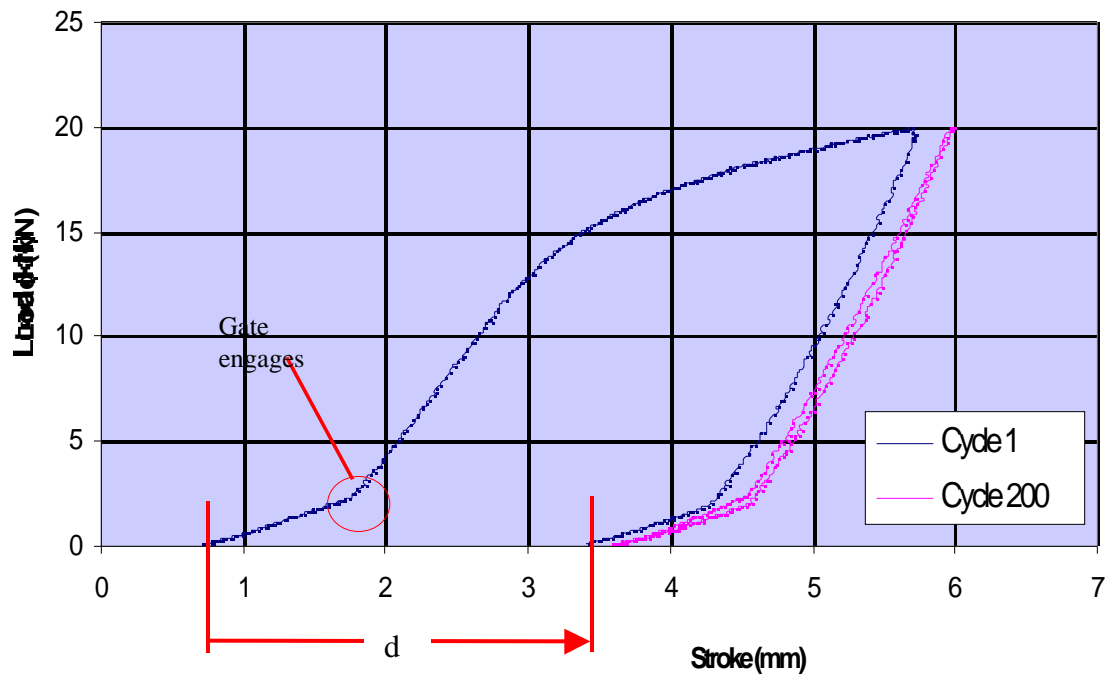


Figure 5. Load vs. Stroke for first and 200th cycle of 0.5 - 20kN test. d , equal to 2.7mm, is the amount of plastic deformation that occurred in the first cycle.

For lower load cycles, the data showed that the carabiners experienced nearly elastic behavior throughout the middle range of the carabiner's lifetime. Figure 6 depicts the difference in stroke between cycle 233 and cycle 9291 of an 8kN test.

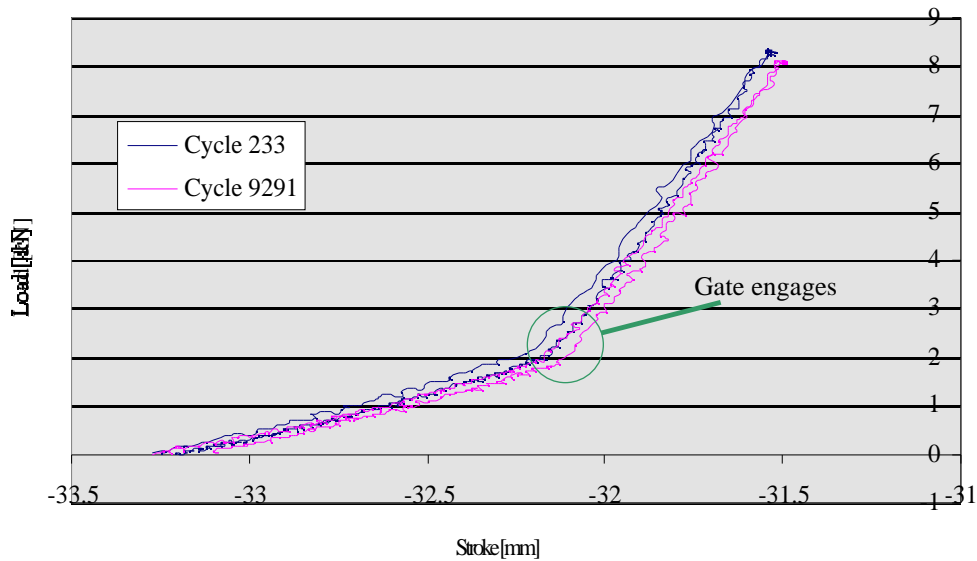


Figure 6. Load vs. Stroke for 233rd and 9291st cycles of a 0.5-8kN cyclic test. No significant plastic deformation is apparent in these stages of the cycling.

Finally, the strain gauge data collected from the spines of 8 and 20kN cycled carabiners also showed plastic deformation at the higher loads and nearly elastic deformation in the mid-lifespan of the carabiners at lower loads. These results are shown in Figures 7 and 8, respectively. Figure 7 also features the sudden decrease in strain the carabiner experiences after being loaded past approximately 8kN. This is hypothesized to be due to the bending of the elbows, which relieve some of the stress from the spine and therefore results in a lower strain in the spine.

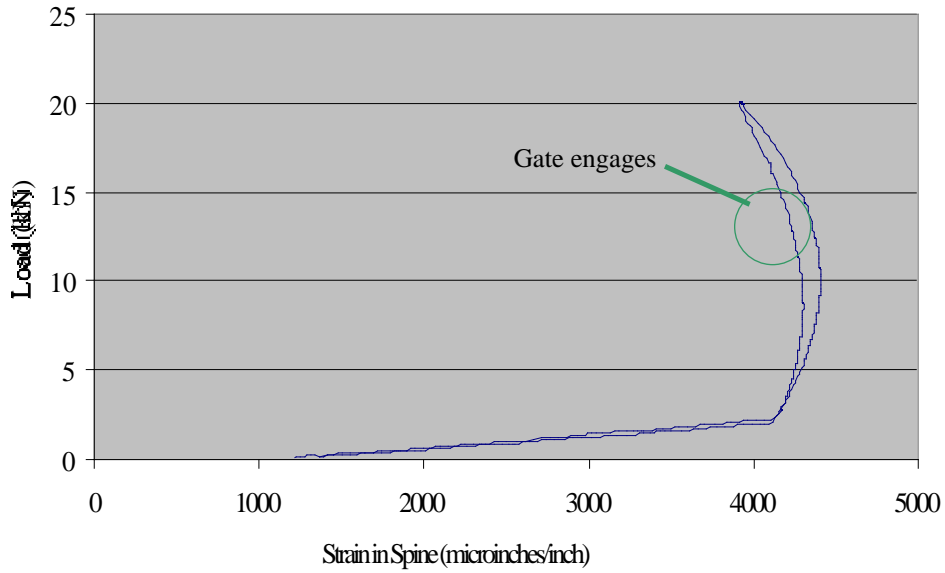


Figure 7. Load vs. strain for cycle 27 of a 20kN cyclic test.

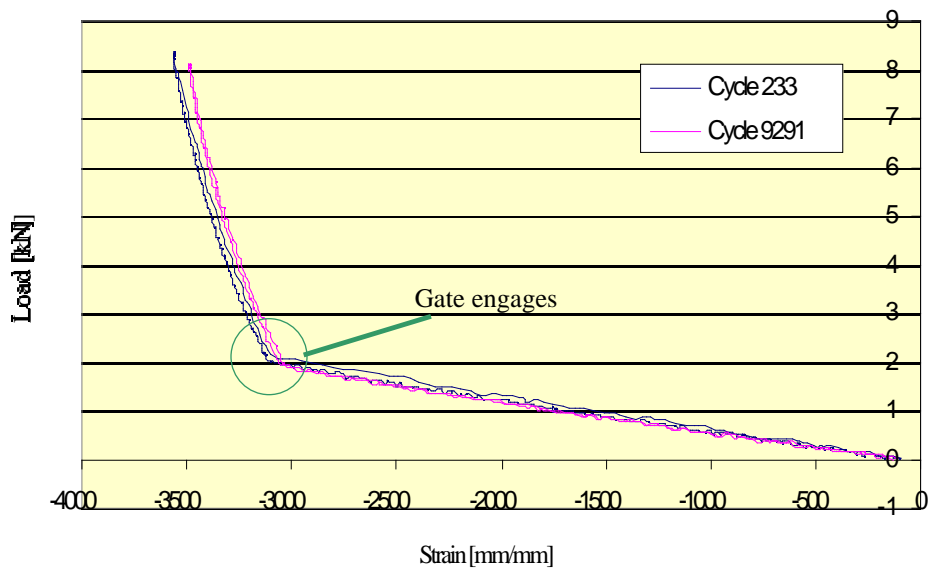


Figure 8. Load vs. strain for cycles 233 and 9291 of an 8kN cyclic test.

Errors due to the deformation of the steel pins were negligible (see Appendix B).

6.4 Fracture Surface Analysis

Carabiners at 8kN were X-rayed to observe surface crack formation. It is difficult to predict the exact lifetime of a carabiner as there is a large variation in the data, and for this reason, it was extremely difficult to approach the very end of a carabiner's lifetime without overshooting. The cycles to failure for the 8kN load case ranged from 9554 to 12775 cycles, and so once the carabiners reached 9000 cycles, they were X-rayed approximately every 500 cycles until failure. In one such test, the last X-ray photograph was taken at 10291 cycles, and the carabiner failed at 197 cycles later. This X-ray, the one taken with the smallest number of cycles prior to failure, did not show any cracks in the carabiner.

Despite the inability to observe cracks before failure, the fracture surface yielded a clear indication of the crack growth in the carabiners. Two pictures of these fracture surfaces are shown below in Figures 9a and 9b. The crack surface can be distinguished by the lighter silver half-moon shaped area at the top of each picture, which is formed as the cracked surface area is polished by the continuous loading.

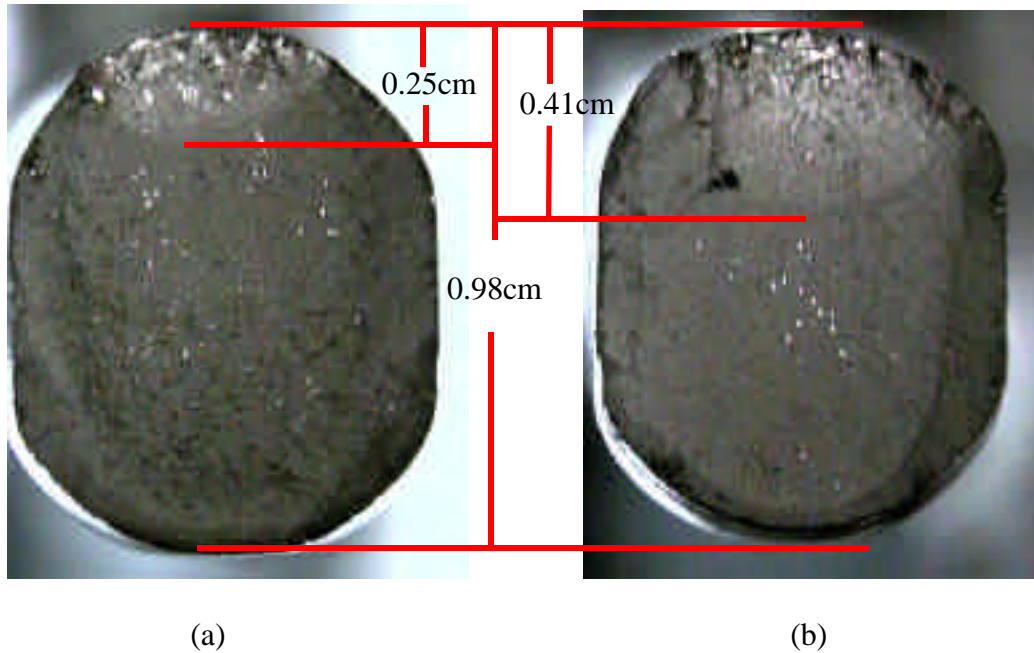


Figure 9. Carabiner fracture surfaces for 12kN (a) and 8kN (b) load cycles. Magnification = 5x.

The length of the crack size, a , for each broken carabiner was determined by using a micrometer and measuring the maximum span of the crack. This data plotted against the stress to determine the relationship between the two, and is shown in the graph in Figure 10.

An interesting observation made in the failure of the carabiners was that all carabiners broke at either elbow (see Figure 1). This is not only consistent with observed in-field failure of carabiners⁹, but also agrees with Finite Element Model analysis predictions (consult Appendix C).

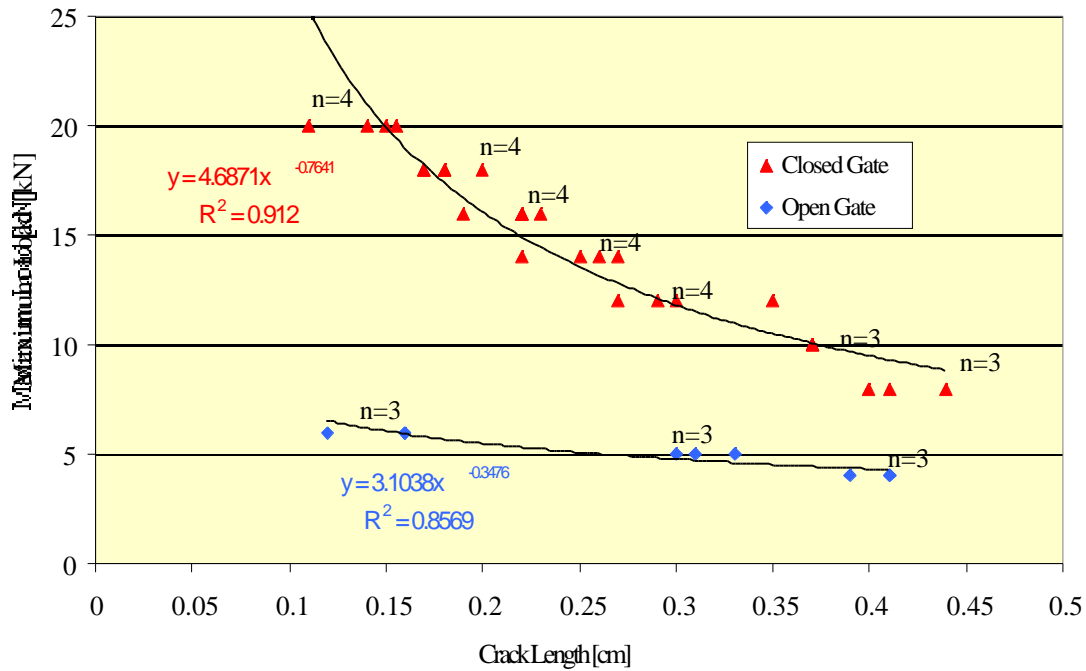


Figure 10. Stress vs. Crack Length for both open and closed gate testing. n = number of tests conducted.

7 Discussion

7.1 Cyclic Testing

Results of the fatigue tests for the carabiners showed that even at very high loads, carabiners are designed to last a long time. The shortest lifetime observed was 194 cycles at a 20kN cyclic load range, or at 83% of the maximum load the carabiner can carry. These results should be very encouraging to climbers because 20kN falls are the worst-case conditions, and therefore rare in the field. In other words, it is very unlikely for a climber to take two hundred 20kN falls in his or her lifetime.

However, most carabiner failure occurs under open gate conditions¹. At these conditions, the shortest lifetime observed was 1309 cycles at 6kN, which represents 86% of the maximum load (7kN) the carabiner can carry. If the load experienced by the carabiner remains below 7kN, these results suggest that the carabiners will last a long time and are safe to use.

7.2 Deformation

It was previously thought that the carabiners would experience a significant deformation in the gate gap. However, the results showed that the deformation in the gate gap was not significant, and, in general, that any deformation was too small to observe with the naked eye.

Most of the observed carabiner deformation occurred in the first few cycles of loading, also contrary to assumptions made at the beginning of the study. From these results, it is hypothesized that a carabiner becomes work hardened in these first few cycles, but further testing must be carried out to support this hypothesis.

These general trends in the deformation of the carabiner conclude that a carabiner's failure cannot be predicted by the deformation characteristics observed in this study. It may be possible that there is significant deformation just before a carabiner fails, but as the latest measurements or short-exposure X-ray photographs were taken just under 200 cycles before failure, this behavior was not observed.

7.3 Fracture Surface Analysis

Long exposure X-ray photographs taken to monitor a carabiner’s crack formation showed no signs of such crack growth up to 197 cycles before failure. Thus, it is possible that the carabiners do not experience crack initiation up to 200 cycles before failure. However, the highly polished crack surface indicates earlier initiation.

The observations made on the fracture surface of the carabiners provided information about the final, or critical crack length. Theory suggests that the relationship between the stress, σ , and the critical crack length, a , is $k_c = \sqrt{\pi a}$, where the constant k_c is the critical stress intensity factor¹⁰. Hence, the relationship between the stress and crack size should theoretically follow an inverse square root behavior:

$$\sigma = \frac{k_c}{\sqrt{\pi a}} = C_1 a^{-0.5} \quad \text{where } C_1 \text{ is the constant } \frac{k_c}{\sqrt{\pi}}$$

However, the exponential relationships found, presented in Section 6.4, behaved as follows:

Table 4: Stress/crack size relationships for open and closed gate conditions.

Closed Gate	Open Gate
$\sigma = 4.69a^{-0.76}$	$\sigma = 3.10a^{-0.35}$

The behavior is significantly different from the model.

In addition, the value of k_c for 7075 aluminum is approximately 24 MPa $\sqrt{\text{m}}$. However, the values for k_c , shown in Figure 11, vary widely, especially between the open and closed gate cases.

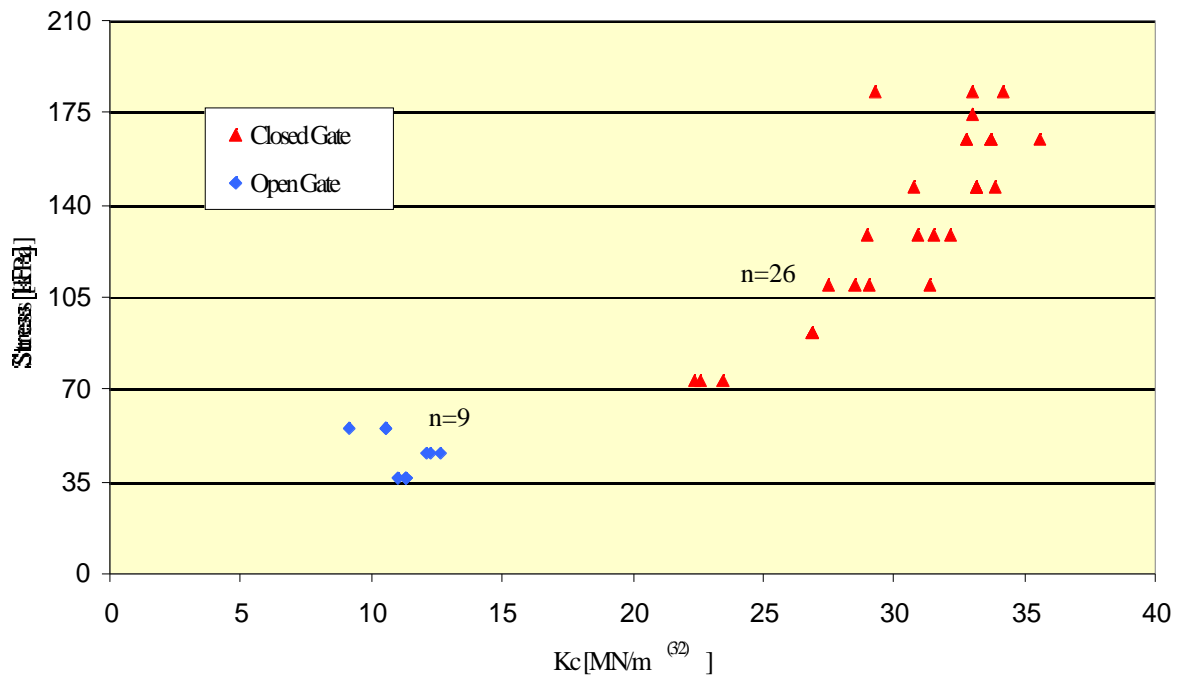


Figure 11. Kc vs. Stress values for both open and closed gate conditions. n = number of carabiners tested.

There is also a large variation within the closed gate case, which ranges from 22.3 to 35.6 MPa m.

These disparities, as well as the differences between theory and model in the equations relating stress to crack area, arise from the assumptions in the model $k_c = \sqrt{\pi a}$. This equation is based on a plane strain problem, or one in which the equations are derived assuming the test specimen to be a long prismatic body in which the length of the object is much greater than the other 2 dimensions (width and thickness)¹⁰. Carabiner spines may come relatively close to such a shape, but the fracture surface is on the elbows, the part of the carabiner that bends the most and resembles a long prismatic body

the least. Hence the discrepancies between the loading conditions at the failure surface and those assumed in the model are likely to be the cause for the disagreement.

7.4 Proposed Fatigue Testing Standard

The current testing standard tests and rates carabiners by a single pull to failure³, a condition rarely met in the field⁹. The results of this study suggest the development of a new fatigue testing standard that reflects the way they are used in the field.

In designing a new test standard, the following key concepts are proposed. First, the testing will involve loads that represent in-field loads, specifically those loads to which the carabiners were subjected. These loads are suggested as they are in the upper end of the range of loads, representing the worst-case scenarios. Also, testing time can be costly to companies, and cycling carabiners below loads of 8kN will, as projected by the L-N curve found in Section 6.2, require over two hours of testing *per carabiner*. The second key concept is to maintain the current industry practice where necessary and useful. For example, the test apparatus used to test carabiners, both in the industry and in this research study, should remain in the new test standard as this design is ASTM approved and already met by many companies.

By using the trend line for the L-N curve found in Section 6.2 and factoring out the 1.2 safety of factor used by a large portion of the climbing industry², a new margin of safety line is obtained. This safety line is depicted in Figure 12 for only the closed gate data of Black Diamond Light D carabiners. It is important to note that each company and each carabiner type within that company will have a different trend line and that the testing standard should be based upon that trend line and applying a factor of safety.

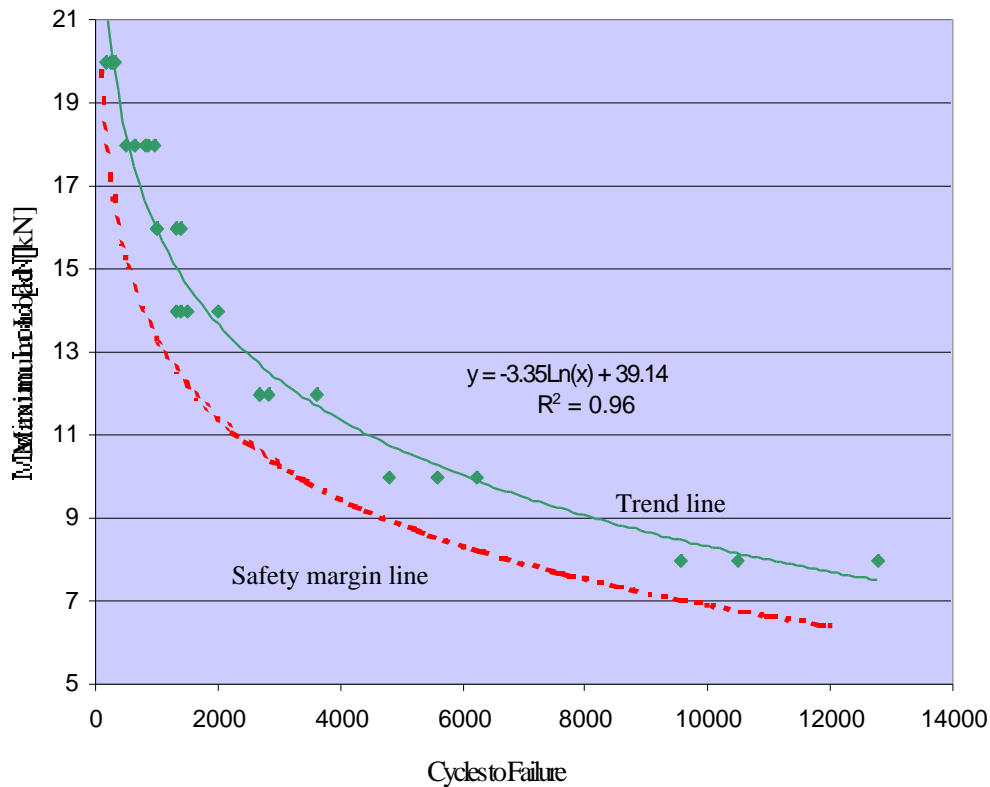


Figure 12. Proposed safety margin line for closed gate testing for Black Diamond Light D carabiners.

The proposed testing standard would call for all carabiners cycled at a certain load to fail at cycles of greater value than of the corresponding value on the safety margin (red) line.

8 Conclusion

A number of conclusions were made about the results discussed above. Under cyclic, dynamic loads such as those experienced in the field, it was found that carabiners have a long lifetime. At the worst-case scenario loading cycle, 0.5-20kN, the shortest lifespan observed was 194 cycles.

Carabiner deformation was not observed by the naked eye. However, the most significant carabiner deformation observed took place in the first few cycles of loading. Because no deformation was observed at the end of any carabiner's lifetime, no predictions were made as to when a carabiner may begin to grow a crack, when it may break, or when it is no longer safe to use.

Furthermore, the observed relationship between crack size, the number cycles to failure, and the stress of the system suggest that a new model for carabiners be developed to accurately describe carabiner crack growth and failure.

Finally, the results of this study have led to a proposed new fatigue testing standard for carabiners.

8.1 Future Work

These results have opened a number of possibilities for continued work in this field. Perhaps one of the most puzzling results is that the greatest amount of plastic deformation in the carabiners occurred in the first few cycles of loading. Further work in this area, specifically in developing a method to characterize carabiner plastic deformation, could perhaps point to the development of a mechanism to inform climbers of at what point in a carabiner's deformation it is no longer safe to use.

Another suggestion for future work is in the determination of crack growth rate in the carabiners. This can easily be done by loading the carabiner a certain number of cycles and then pulling it apart in a single pull. Thus, if a crack has formed during that period, it will appear on the fracture surface, as shown in Figure 9. The test can be repeated for various numbers of cycles to establish crack growth rate.

Additionally, climbers take falls of a variety of magnitude onto their carabiners, and studying the effects of a large fall on the carabiner lifetime could point to useful results. This can be observed by loading the carabiners with one large load, such as 20kN, then cycling the carabiner to failure at a much lower loads, such as 8kN.

Finally, all 35 carabiners tested broke at the elbows. The design of a carabiner with reinforced elbows may lead to stronger, safer carabiners.

References

1. Graydon & Hanson, *Mountaineering: Freedom of the Hills*. 6th Edition.
2. Soles, C. Gear; Equipment for the Vertical World. The Mountaineers Books, Seattle, WA, 2000. pp. 33.
3. Anon. *Standard Specification for Climbing and Mountaineering Carabiners*, ASTM Designation F1774-97. Annual Book of ASTM Standards, November, Vol. 15, 1998.
4. Pavier, M. "Experimental and Theoretical Simulations of Climbing Falls." *Sports Engineering*, pp. 79-91, January 1998.
5. Walk, M. "Strain/Displacement of a Carabiner via Interferometry." *Laser Interferometry X: Applications*, pp. 409-17, Vol. 4101, 2000.
6. McLean, A. "Beauty and the Biner." Black Diamond Equipment Catalogue, pp. 67. Spring 2001
7. Kane, John. Personal Communication on 4/11/01.
8. As found on the following website:
http://216.46.227.18/articles/interpret/Analyzing_one_group/descr_stats.htm
9. Custer, Dave. Personal Communications on 3/2/01.
10. Fuchs & Stephens. *Metal Fatigue in Engineering*. pp 37-39, 46-52.
11. Crandall, Dahl, & Lardner. *An Introduction to the Mechanics of Solids*. 2nd Edition.

Appendix A – Engineering Drawings

The full dimensions of the four components of the total ASTM grip set-up are shown below. All dimensions are given in inches as the machinery in the Gelb Laboratory operates with English units.

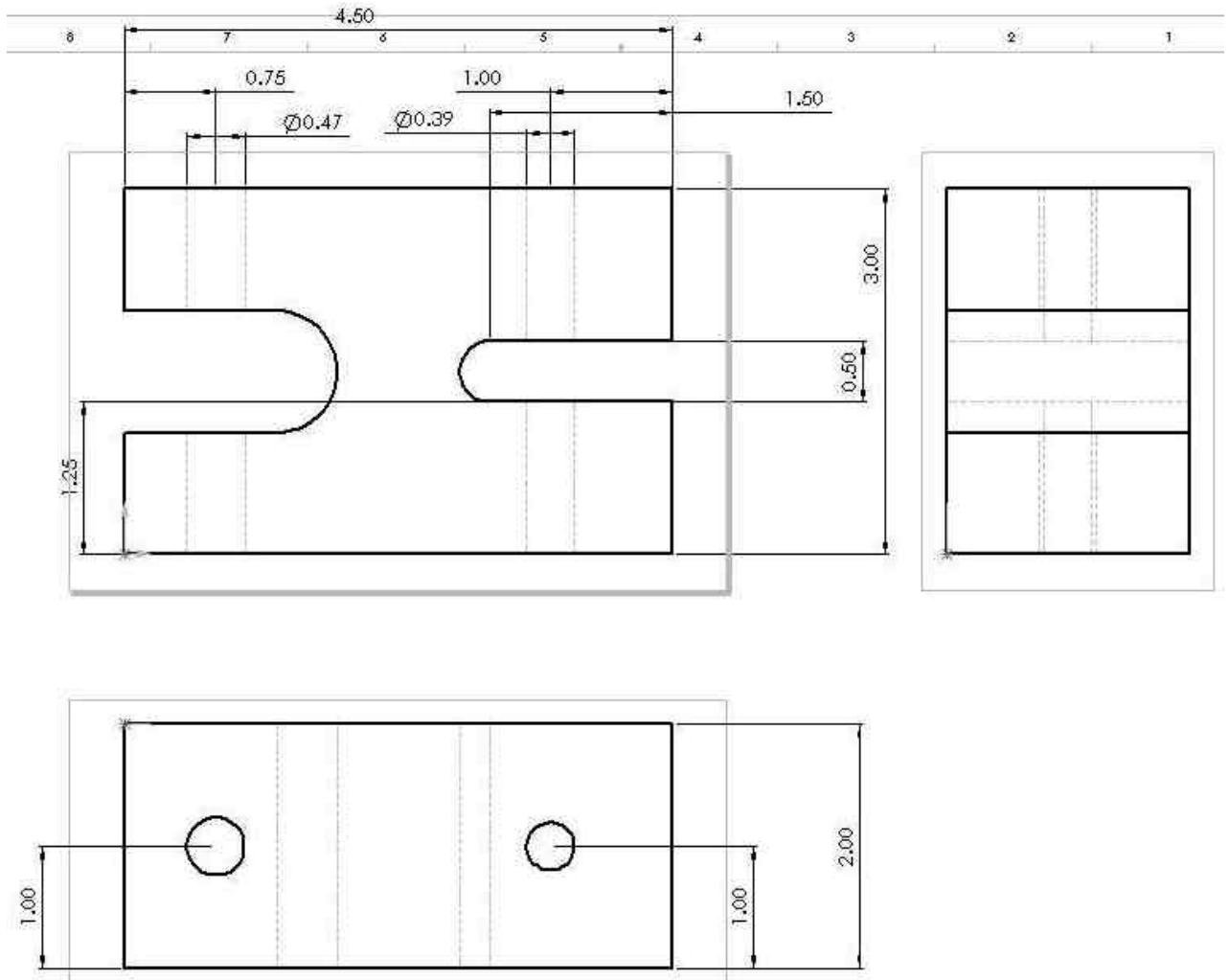


Figure A-1. Three-view of main ASTM grips.

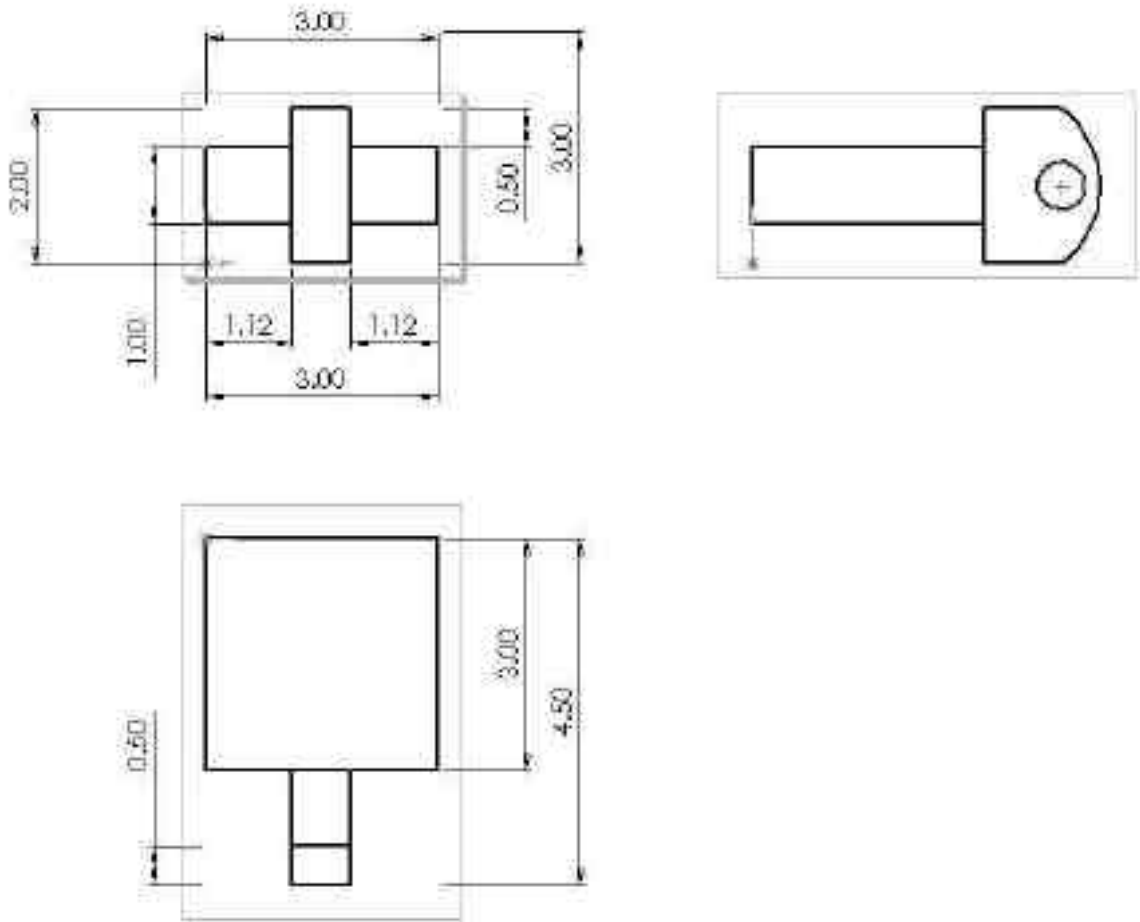


Figure A-2. Three-view of the connectors.

Appendix B - Error Analysis

The errors associated with these results are mostly associated with the measurements that were taken throughout the testing. The greatest source of error lies in the MTS loading machine, which is accurate to $\pm 13\text{N}^7$. Since the carabiners experienced loads from 8 to 20kN, at most this inaccuracy represented a $13/8000$, or 0.163% error in the loading of the carabiner.

Another source of error accounted for in the MTS displacement reading is due to the deformation in the steel dowels during loading. The pin is loaded vertically by the carabiner, as shown in Figure B-1(a) and can be modeled by the free body diagram in Figure B-1(b)¹¹.

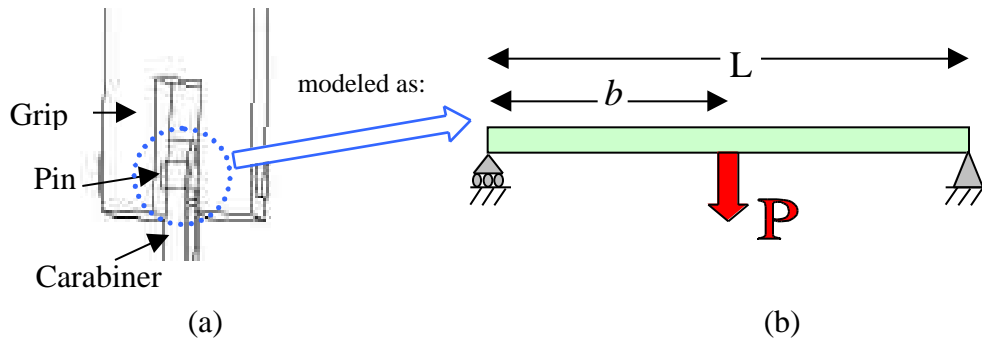


Figure B-1: Pin/carabiner free body diagram.

The maximum deflection for this system is¹¹

$$\delta_{\max} = \frac{Pb(L^2 - b^2)^{3/2}}{9\sqrt{3}LEI}$$

The maximum error, e_{\max} , is defined as $100 \frac{\delta_{\max}}{w_{\min}}$, where δ_{\max} is the maximum deflection in the pin and w_{\min} is the minimum deflection observed and obtained from computer output. The following worst-case scenario values were used to determine e_{\max} :

$$P = 24 \text{ kN (single pull)}$$

$$b = \frac{1}{2} L$$

$$E = 70 \text{ GPa}$$

$$I = \frac{\pi}{4} r^4 = 9.82e-10 \text{ m}^4$$

These values yielded $\delta_{\max} = 4.97e-6$ meters, and the smallest observed deflection was 0.0015 mm. Hence, $e_{\max} = 100 \frac{\delta_{\max}}{w_{\min}} = 100 \frac{4.97e-6}{1.5e-3} = 0.33\%$ and was considered to be

negligible.

Errors in the installation of the strain gauges onto the carabiners were corrected by calibrating the gauges before loading. Gauge errors from electric noise and interference in the testing environment and thermal effects were assumed to be negligible⁷.

Finally, carabiner manufacturing error is negligible, as all major distributors assure a Three Sigma rating on breaking strengths for their carabiners⁶.

Appendix C - Finite Element Model of Carabiner Failure

In the spring of 2001, a finite element analysis was performed on a 3-D model of a carabiner in order to predict the carabiner's location that would be most likely to break under loading. The software used to develop the model was PATRAN, and the finite element analysis tool used was NASTRAN. The stress data, shown in Figure 12, indicated that the carabiner would fail at the elbow, which was consistent with data observed in the field¹¹.

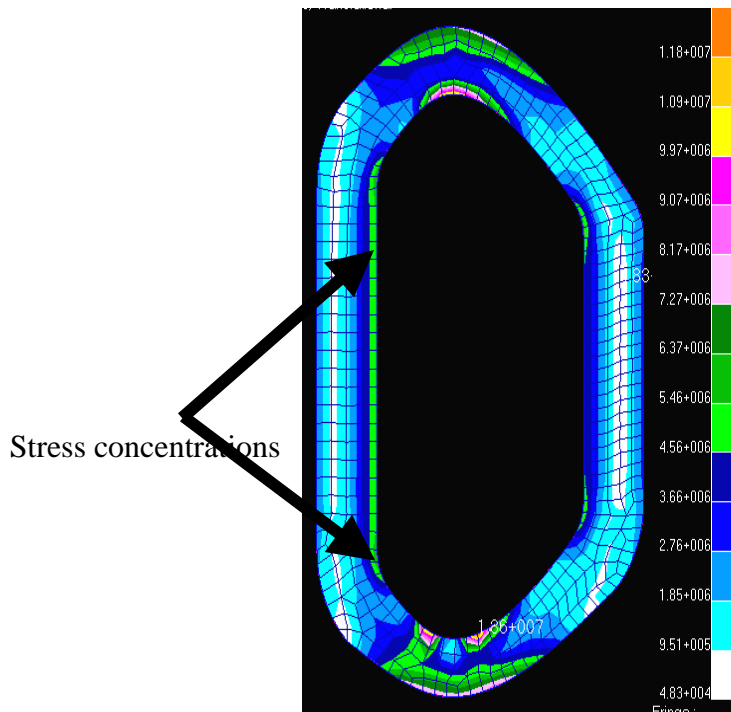


Figure C-1: Finite element analysis of a D-shaped carabiner. Major stress concentrations are located at either end of the carabiner (due to PATRAN model configurations) and the elbows, where carabiners have been known to fail in the field.

Hence, a fatigue failure estimation of the elbow using an S-N curve (Stress vs. Number of cycles to failure) was attempted by modeling the elbow as a straight rod¹². The S-N curves in the Military Handbook for an Aluminum 7075 straight rod predicted failure at 10^7 cycles at the low end of the load range, or 8 kN, and on the order of 10^5 cycles at the high end of the range, or 24 kN. However, carabiners are rated at the force at which they fail under a single, tensile pull, and this number is usually 24 kN. This implied that it would only take one cycle for a carabiner to break at a 24 kN and that the S-N curve predictions were too conservative to adequately model the elbow. It was therefore assumed that the carabiners would require on the order of 10^4 cycles at all ranges as a conservative approach to the required laboratory time. Thirty-three carabiners were to be tested at a period of 0.5 seconds, implying the total MTS machine test time would be;

$$\frac{10^4 \text{ cycles} \quad 33 \text{ carabiners}}{2 \text{ cycles / second} \quad 3600 \text{ seconds / hour}} = 45 \text{ hours}$$

Appendix D - Raw Data

Table D-1: Raw Data Collected on Carabiners

Max. Load [kN]	Cycles to Failure	Crack Length [cm]	Biner dims. d (height)
20	255	0.14	0.0098
20	194	0.15	h (width)
20	312	0.11	0.00835
20	289	0.155	
18	489	0.18	Biner area
18	826	0.17	[m ²]
18	845	0.18	1.09E-04
18	950	0.2	
18	642	0.17	
16	989	0.23	
16	1020	0.22	
16	1408	0.22	
16	1310	0.19	
16	2526	0.22	
14	1988	0.25	
14	1386	0.26	
14	1509	0.27	
14	1340	0.22	
12	2688	0.27	
12	3608	0.29	
12	2693	0.3	
12	2844	0.35	
10	5588	0.37	
10	6226	0.37	
10	4785	0.37	
8	10488	0.41	
8	12775	0.44	
8	9554	0.4	
6	1916	0.16	
6	2098	0.16	
6	1309	0.12	
5	3339	0.33	
5	2972	0.31	
5	3740	0.3	
4	6901	0.39	
4	9694	0.41	
4	6952	0.41	